Sains Malaysiana 54(11)(2025): 2721-2731
http://doi.org/10.17576/jsm-2025-5411-12

Distinct Degradation Behaviors of Gaseous H_2O_2 and Benzene in NaOH-$MnSO_4$, MnO_2, and KI Systems

(Kelakuan Degradasi Berbeza bagi Gas H_2O_2 dan Benzena dalam Sistem NaOH-$MnSO_4$, MnO_2 dan KI)

YUPING JIANG*, ANDONG ZHU & SHIMIN WU

University of Electronic Science and Technology of China, Zhongshan Institute, China

Received: 23 May 2025/Accepted: 7 November 2025

ABSTRACT

Gas-phase H_2O_2 ($[H_2O_2]_g$) degradation is crucial yet insufficiently characterized, particularly under pollutant coexistence conditions. This study innovatively investigates the degradation behaviors of $[H_2O_2]_g$ and $[benzene]_g$ using NaOH-$MnSO_4$ solution, MnO_2 catalyst particles, and KI solution systems. Experimental results demonstrate: fluorinated ethylene propylene (FEP) materials effectively mitigate system transfer losses. Under both isolated and coexisting conditions, NaOH-$MnSO_4$ and KI solutions maintained high $[H_2O_2]_g$ degradation efficiency (>90%). However, KI's $[benzene]_g$ removal rate plummeted from 14% to 4%, while competitive $[benzene]_g$ adsorption reduced MnO_2's $[H_2O_2]_g$ removal efficiency from 90% to 52%, with $[benzene]_g$ removal remaining constant. A unique anti-synergistic effect was identified in the NaOH-$MnSO_4$/MnO_2 system, hypothesized to result from rapid hydroxyl radical annihilation under high alkalinity and H_2O_2 concentration. Cross-validated pH monitoring and UV-Vis spectroscopy suggest H_2O_2-induced iodide depletion in the KI system substantially weakens hydrogen bond-mediated benzene solubilization. Spectral analysis further showed excessive H_2O_2 masks benzene's characteristic peaks, while emerging absorption bands confirm intermediate product formation during oxidation.

Keywords: Benzene; hydrogen peroxide; hydroxyl radical; removal efficiency; synergistic effect

ABSTRAK

Degradasi H_2O_2 ($[H_2O_2]_g$) fasa gas adalah penting tetapi tidak dicirikan dengan secukupnya, terutamanya di bawah keadaan kewujudan bersama bahan pencemar. Penyelidikan ini secara inovatif mengkaji tingkah laku degradasi $[H_2O_2]_g$ dan $[benzena]_g$ menggunakan larutan NaOH-$MnSO_4$, zarah pemangkin MnO_2 dan sistem larutan KI. Keputusan uji kaji menunjukkan bahan etilena propilena (FEP) berfluorinasi berkesan mengurangkan kehilangan pemindahan sistem. Di bawah kedua-dua keadaan terpencil dan wujud bersama, larutan NaOH-$MnSO_4$ dan KI mengekalkan kecekapan degradasi $[H_2O_2]_g$ yang tinggi (>90%). Walau bagaimanapun, kadar penyingkiran $[benzena]_g$ KI menurun mendadak daripada 14% kepada 4%, manakala penjerapan $[benzena]_g$ yang kompetitif mengurangkan kecekapan penyingkiran $[H_2O_2]_g$ MnO_2 daripada 90% kepada 52% dengan penyingkiran $[benzena]_g$ kekal malar. Kesan anti-sinergi yang unik telah dikenal pasti dalam sistem NaOH-$MnSO_4$/MnO_2 yang dihipotesiskan sebagai hasil daripada pemusnahan radikal hidroksil yang cepat di bawah kealkalian yang tinggi dan kepekatan H_2O_2. Pemantauan pH yang disahkan silang dan spektroskopi UV-Vis menunjukkan bahawa penipisan iodida yang disebabkan oleh H_2O_2 dalam sistem KI secara ketara melemahkan pelarutan benzena yang dimediasi ikatan hidrogen. Analisis spektrum selanjutnya mendedahkan H_2O_2 yang berlebihan menutupi puncak ciri benzena, manakala jalur penyerapan yang muncul mengesahkan pembentukan produk perantaraan semasa pengoksidaan.

Kata kunci: Benzena; hidrogen peroksida; kecekapan penyingkiran; kesan sinergi; radikal hidroksil

INTRODUCTION

Hydrogen peroxide (H_2O_2) is widely known as an important species in air, can participate in atmospheric reactions, such as oxidizing SO_2 to SO_3 (Li, Simon & Jonathan 2020), affecting the global radiation budget and causing acid rain deposition (Li et al. 2021a). At present, oxidants and other key impact factors including $[H_2O_2]_g$ are still not reduced to the same extent as many pollutants (Möller 2009). $[benzene]_g$ and its derivatives can be widely used as organic liquids in multiple industries, such as extracting chemicals (Kumar, Holuszko & Janke 2020), is most dangerous gas for the atmosphere (Singh, Singh & Mishra 2019). Moreover, benzene oxidation and hydrogen peroxide decomposition are kinetically linked (Kaur, Singh & Aggarwal 2024). Obviously, decreasing $[H_2O_2]_g$ and $[benzene]_g$ is favourable for advancing air quality. It is a well-known fact that H_2O_2 can be decomposed through oxidation of KI. Alkaline solutions

(Xu et al. 2018) and manganese-based catalysts are also effective systems for H_2O_2 decomposition (Elbasuney et al. 2024; Liu et al. 2025; Tian et al. 2000). Furthermore, manganese catalysts exhibit dual functionality as both electron donors and acceptors during H_2O_2 decomposition (Möller 2009), demonstrate superior decomposition capability compared to other ionic species and present significant cost-effectiveness advantages (Quentin et al. 2022). MnO_2-based catalytic systems have also been employed for catalytic oxidative degradation of benzene (Chen et al. 2016), with controlled MnO_2 structures and morphologies shown to enhance degradation efficiency (Chen et al. 2023). The decomposition of H_2O_2 typically generates hydroxyl radicals (•OH) that accelerate the degradation of various organic pollutants, including benzene (Fuku et al. 2021). This establishes synergistic effects with the substrate (Kaur, Singh & Aggarwal 2024). H_2O_2 and pollutants always coexist in the atmosphere; for instance, when the oxidation process is applied for pollutant removal, residual H_2O_2 is always emitted with pollution at the same time after the reaction, thus interfering with further treatment or detection (Luan et al. 2021) and competitive adsorption or catalytic interactions exist between $[H_2O_2]_g$ and contaminants (Jiang, Song & Zhu 2021). Specific conditions may amplify the complexity of degradation mechanisms, in which H_2O_2 decomposition may be suppressed under elevated pH conditions (Opeida & Sheparovych 2019), and constrain organic matter oxidation reactions (Zhang, Liu & Lu 2010). These findings highlight the theoretical and practical significance of investigating decomposition patterns in hydrogen peroxide-substrate systems. However, recent research in this domain has declined in frequency, with mechanistic studies exhibiting discontinuous progress, particularly regarding gaseous mixed systems. Building on previous research, this study rationally hypothesizes that innovatively designing the rare $[H_2O_2]_g$-$[substrate]_g$ degradation processes can show distinctive synergistic effects under diverse conditions (including extreme scenarios), thereby refining and deepening mechanistic understanding, which constitutes the primary objective of this investigation. Therefore, this investigation employs a degradation system comprising NaOH-$MnSO_4$ mixture, MnO_2 catalyst particles, and KI solution. Individual and synergistic degradation processes were examined for $[H_2O_2]_g$ and $[benzene]_g$, in which physical and chemical degradation effects were evaluated through pH monitoring and UV-Vis spectroscopy analysis. Accounting for potential physical depletion of $[H_2O_2]_g$ (Li et al. 2021b), the research additionally investigated wet deposition processes during material transport.

MATERIALS AND METHODS

CHEMICALS AND CATALYST

A 30% hydrogen peroxide (H_2O_2) solution, potassium iodide (KI), manganese dioxide (MnO_2) and benzene were used in this study. All chemicals were of analytical grade, purchased from the market and used as received. The catalyst particles were prepared by a homemade method. The cement and MnO_2 powder were mixed according to the mass ratio of 1:8 and stirred (100r/min), while pure water was added to form the paste. Then, particles with a diameter of 1 mm were shaped and dried for more than 24 h. The pellets were analyzed using a surface area and porosity analyzer, showing a specific surface area of 18.5 ± 2 m^2/g and porosity of 38.6% ± 2.3%.

EXPERIMENTAL PROCEDURE

The experimental was conducted in an air-conditioned indoor environment maintained at 23 °C, utilizing the experimental system shown in Figure 1. Air was blown through FEP pipes, which have good light transmittance and small wall loss (Li et al. 2021b), and regulated by rotameters to transfer the benzene and H_2O_2 vapour in A and B, followed by mixing in the E. According to the requirement, KI (0.1 mol/L), $MnSO_4$ (5×10^{-5} mol/L)+NaOH (0.1 mol/L) and MnO_2 catalyst were placed into a 1000 mL reactor (G) separately, the total volume for the solutions and the accumulated particles was 500 mL, and then the $[H_2O_2]_g$ and $[benzene]_g$ was removed. The initial concentrations of reactants were measured through the gas at the pass line (C and D), inlet and outlet of G through F and H, separately. Reactants were sampled directly in G to determine the pH and UV–Vis absorption, as required.

ANALYSIS

H_2O_2 was sampled through an atmospheric absorption bottle and then measured by the iodometric method described elsewhere (Wang 2012). The $[benzene]_g$ concentrations were monitored via gas chromatography (GC) with FID and AB-INOWAX fused silica capillary columns with a retention time of 1.2-1.6 min; pH was investigated using an acidimeter (Model Starter 2100/3C Pro, Shanghai Hongji Instrument Co., Ltd. China) every 10 min and UV–vis absorption was measured using a NanoDrop Lite UV–Vis Spectrophotometer. All experiments were conducted in triplicate with averaged results (relative error between triplicate measurements and means ≤2%), For transport effect measurements exhibiting larger relative errors, data were averaged from 10 repeated measurements. Transport loss rate and removal efficiency were calculated using Equations (1) and (2).

$$Loss\ rate\ (\%)=(C_{initial}-C_{inlet})*100/C_{initial} \quad (1)$$

$$Removal\ efficiency\ (\%)=(C_{inlet}-C_{outlet})*100/C_{in} \quad (2)$$

where $C_{initial}$, C_{inlet}, and C_{outlet} are the initial, inlet and outlet concentrations of H_2O_2 or benzene sampled in C (D), F and H, respectively.

RESULTS AND DISCUSSION

THE EFFECT ON TRANSPORTATION

Because a 1 m FEP pipe with good light transmittance was used, the possible reactant loss by transportation was also explored in this study, and the results are shown in Figure 2. It is obvious that for all the different conditions, the maximal loss for $[H_2O_2]_g$ reaches 1% after transportation. This small value can be ignored within the error range. Although $[H_2O_2]_g$ has a loss effect due to wet deposition (Chen et al. 2020), for transportation, it is appropriate to select FEP materials due to its strong physicochemical stability and light transmittance. Additionally, benzene demonstrated substantially lower loss rates than $[H_2O_2]_g$ under both isolated and co-transport conditions, indicating its superior chemical stability compared to $[H_2O_2]_g$. Figure 2 also show that individual transport of $[H_2O_2]_g$ and benzene showed lower and higher loss rates, respectively, compared to their co-transport. This phenomenon may be attributed to $[benzene]_g$'s dual roles: as the component in the gas mixture, it reduces $[H_2O_2]_g$ concentration and thereby slows its decomposition rate, while its aromatic ring structure potentially forms weakly bound states with H_2O_2 molecules through π-π interactions or other non-covalent forces to minimize peroxide loss (Xuan et al. 2020). Paradoxically, benzene's molecular framework may also trap free radicals (hydroxyl radicals) generated during $[H_2O_2]_g$ decomposition, thereby suppressing peroxide breakdown while unexpectedly increasing benzene's own loss rate. This confirms the previous hypothesis that the co-degradation process of $[H_2O_2]_g$-$[substrate]_g$ produces synergistic effects, while further showing the existence of physical synergistic mechanisms. It is particularly noteworthy that the experiment utilized small-diameter tubing (15 mm) with a short-length configuration (1 m), where gas flow rate control maintained a gas residence time of approximately 1.2 s, thereby significantly mitigating the risk of material loss during transport.

REMOVAL OF $[H_2O_2]_g$

The performance of $[H_2O_2]_g$ degradation was investigated without $[benzene]_g$, as shown in Figure 3. All the

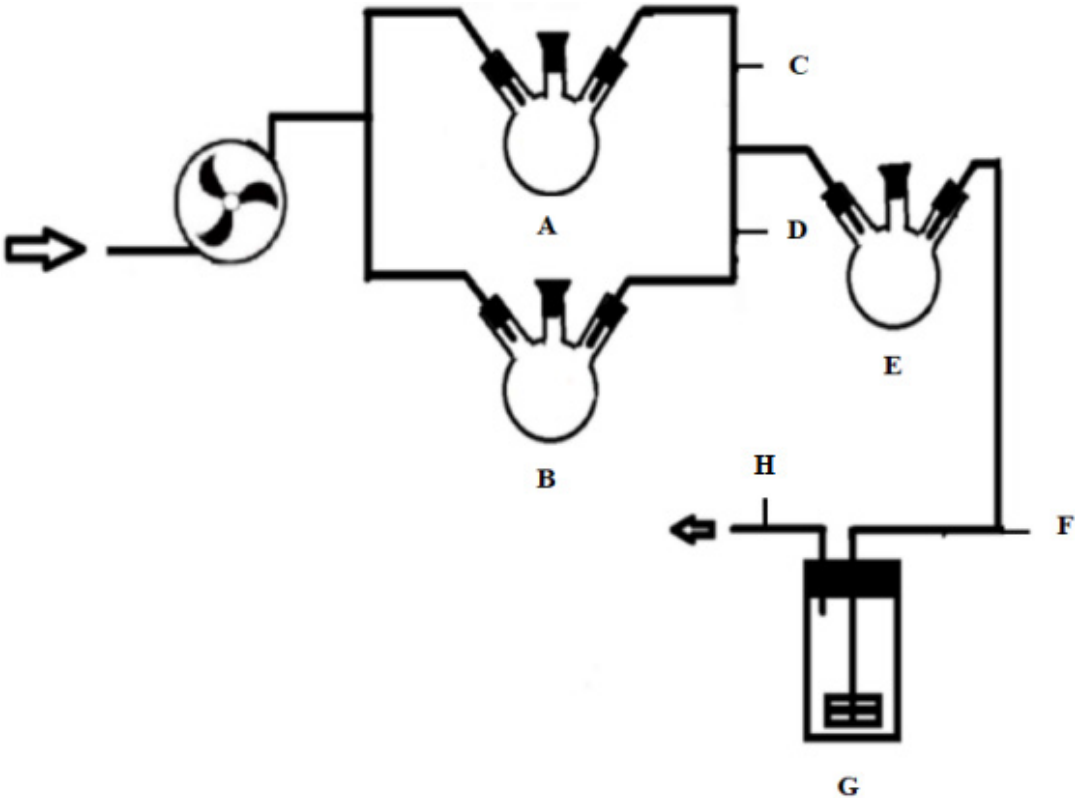

FIGURE 1. Schematic of the experimental system. A-Container with H_2O_2 solution; B-Container with liquid benzene; C-Sampling port for the initial $[H_2O_2]_g$ concentration; D-Sampling port for the initial $[benzene]_g$ concentration; E-Mixing container; F-Sampling port for the mixing concentration; G-Reactor, H-Sampling port for the residual concentration

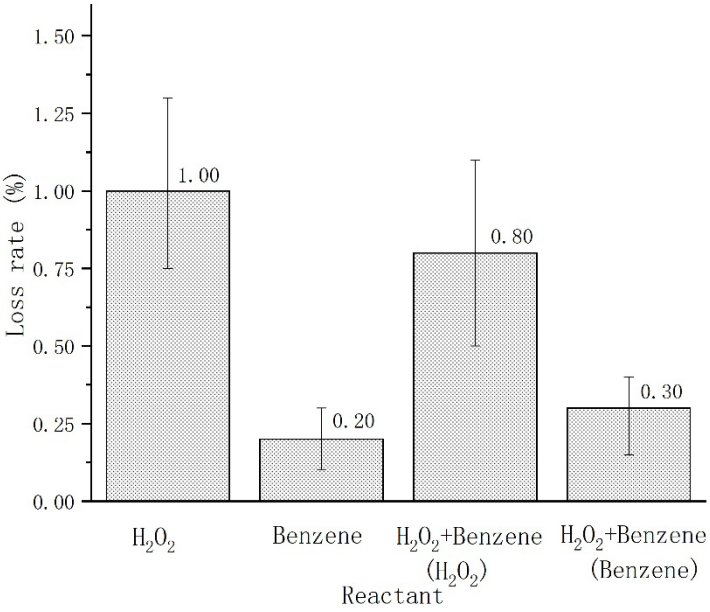

Conditions. The experimental conditions were as follows: $[H_2O_2]_g$ initial concentration, 4.6 mol/m^3; $[benzene]_g$ initial concentration, 630 mg/m^3; gas flow, 9 L/min; reaction temperature (room temperature), 23 °C.

FIGURE 2. The effect of transportation

degradation rates are found to be very good (≥90%). For the KI solutions, due to the alkalinity for the solution, high oxidation–reduction potential (1.8 V) for H_2O_2 and strong reducibility for I^-, the redox reaction between these species naturally occurred to remove the $[H_2O_2]_g$. In a solution of NaOH+$MnSO_4$, the alkalinity was also beneficial to the decomposition of $[H_2O_2]_g$. In addition, Mn(II) could activate peroxide and promoted its decomposition via catalyzed reactions, and the addition of NaOH led to Mn-OH production with a strong catalytic effect (Ma et al. 2020). For catalyst particles, it is believed that an electron exchange reaction between the catalyst surface and H_2O_2 molecules initiated the decomposition, which reduced MnO_2 (Mn oxidation state 4+) to Mn^{3+} via the following reactions (Zhang et al. 2018):

$$Mn^{4+}+H_2O_2 \longrightarrow Mn^{3+}+H^++HO_2\cdot \quad (3)$$

$$HO_2\cdot+H_2O_2 \longrightarrow H_2O+O_2+HO\cdot \quad (4)$$

$$HO\cdot+Mn^{3+} \longrightarrow Mn^{4+}+OH^- \quad (5)$$

Figure 3 also shows that at a reagent volume of 500 mL, both KI solution and NaOH-$MnSO_4$ solution achieve a 94% removal efficiency of H_2O_2, which is significantly higher than the 90% observed with MnO_2 particles. This difference stems from the varying reaction efficiencies between homogeneous (solutions) and heterogeneous (particles) systems. Specifically, the redox reaction between I^- and H_2O_2 in KI solution and the catalytic effect of Mn-OH active species in NaOH-$MnSO_4$ solution are both rapid homogeneous reactions. In contrast, the heterogeneous catalysis of MnO_2 particles relies on electron exchange between surface Mn^{4+}/Mn^{3+} and H_2O_2, with its initial removal efficiency slightly lower due to limitations in gas-solid contact efficiency.

Figure 4 shows that the degradation rate does not increase in the reagent range of 500-1000 mL and then is slowly increased to almost 100% in 1000-2500 mL. This phenomenon is explained by the fact that although the removal mechanisms are different from each other, the efficiency were increased only by increasing the reagent to a certain amount. For MnO_2 particles, under conditions of high substrate concentration and low initial catalyst loading, the limited active sites become rapidly saturated. The system cannot degrade the substrate efficiently due to insufficient contact frequency, resulting in surface saturation and suboptimal efficiency improvement (Kim et al. 2018), the other two systems may induce product accumulation and altered reaction pathways under high concentrations, thereby inhibiting the enhancement of degradation rates. However, increased quantities generate additional active sites and dilution effects, weakening inhibitory effects and elevating degradation rates. Despite a lower initial removal rate, MnO_2 particles exhibited the most pronounced improvement, ultimately achieving a degradation rate close to 100%.

REMOVAL OF BENZENE

As shown in Figure 5, $[benzene]_g$ can slightly dissolve in water, although the solubility is very low. However, it is

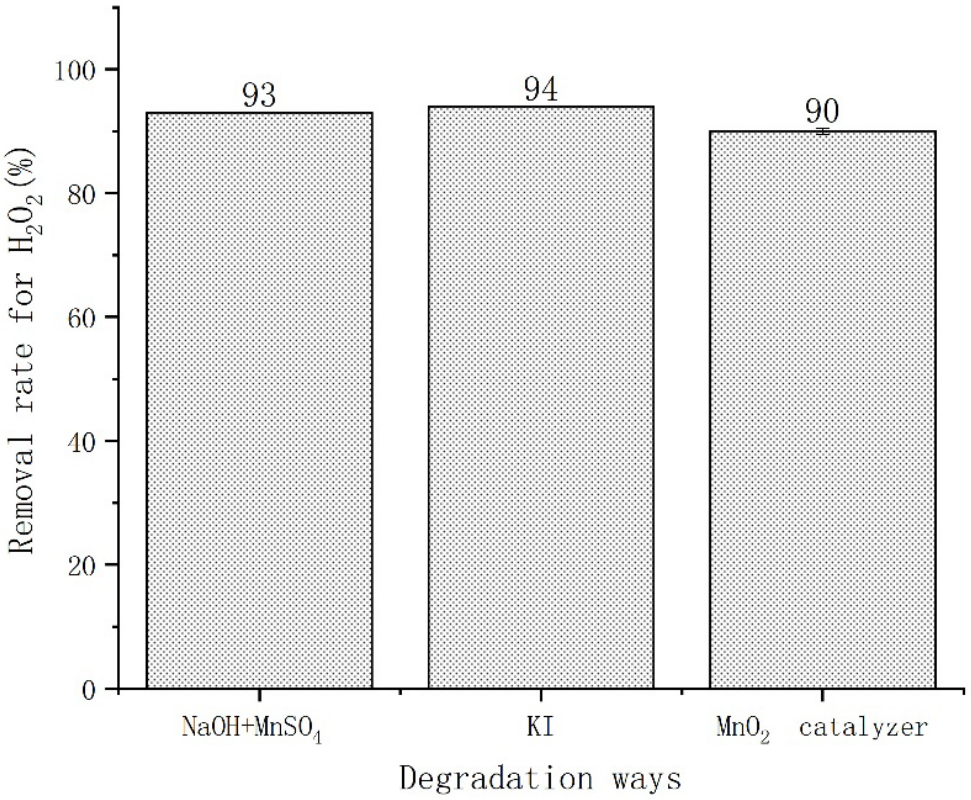

Conditions. The experimental conditions were the same as those used in Figure 1, except for the absence of $[benzene]_g$ and the addition of 500 mL of degradation reagent.

FIGURE 3. Removal of H_2O_2 in different ways

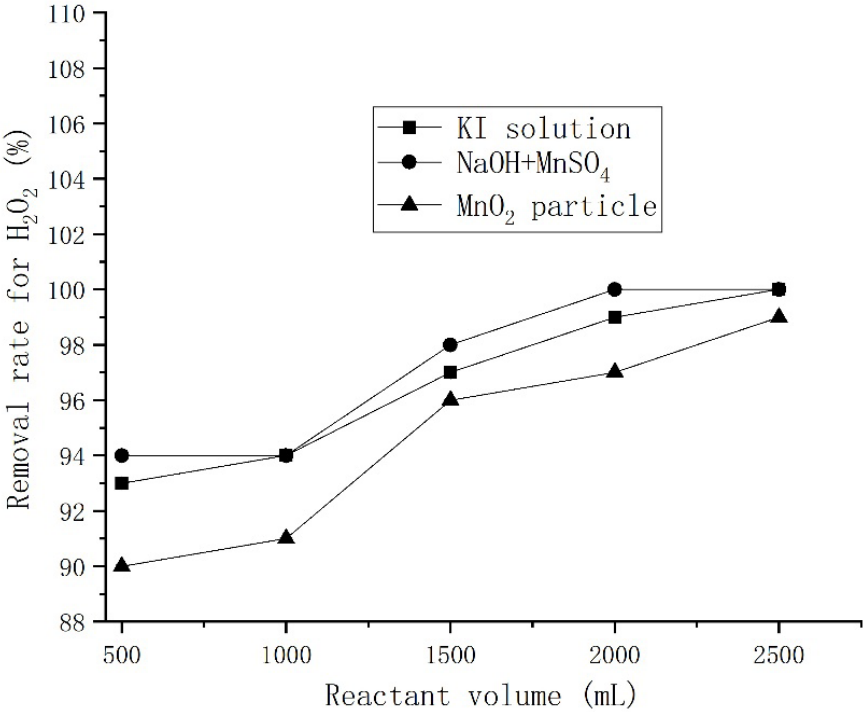

Conditions. The experimental conditions were the same as those used in Figure 2, except for the addition of degradation reagent of different volumes.

FIGURE 4. Effect of reagent quantity

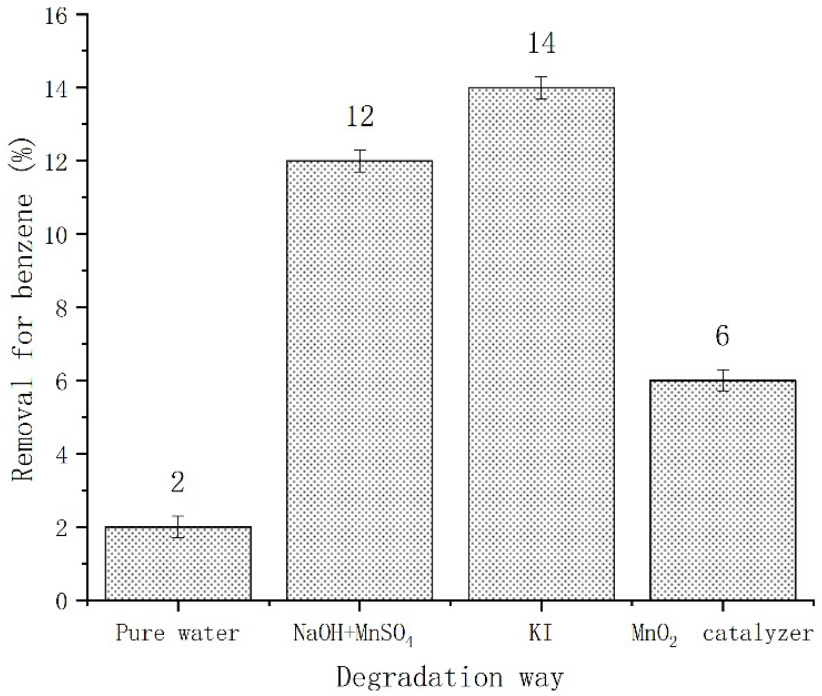

Conditions. The experimental conditions were the same as those used in Figure 1, except for the absence of $[H_2O_2]_g$ and the addition of 500 mL degradation reagent.

FIGURE 5. Removal of benzene in different ways

very interesting that the solubility increases in solutions of NaOH+$MnSO_4$ and KI. Although it was proved that in the polar solution, the solubility of benzene reduced with increasing electrolyte solutions concentration, such as NaCl and Na_2SO_4 (Chen et al. 2023), both the hydrogen bond acceptors and hydrogen bond donors also increased the solubility, especially in the solutions with non-strong acid and alkali, in which the former had a greater effect, especially for the ions with larger radius (Villanueva 2018; Wang et al. 2016). Therefore, in the two solutions for our experiment, the unbalanced polar bond can easily formed hydrogen bonds with aromatic rings or double bonds, which significantly increased the solubility in which I^- was the hydrogen bond acceptor and had a larger volume, easily moved around the cation and interacted with more benzene molecules compared with NaOH+$MnSO_4$. The extremely low benzene removal rate (2%) in pure water can be attributed to the poor compatibility between nonpolar benzene and aqueous systems, coupled with the absence of hydrogen bond acceptors compared to other solutions. For degradation by the MnO_2 catalyst, the lower effect proves that although manganese-based catalysts demonstrate higher efficiency in removing $[H_2O_2]_g$ compared to other metals (Qi et al. 2021), this is also closely associated with hydrogen peroxide's inherent tendency to decompose easily and its strong adsorption onto MnO_2 particle surfaces - both being highly polar substances. In contrast, benzene is a typical nonpolar molecule with a stable aromatic ring structure characterized by a large π-bond system, leading to poor absorbability and high stability. Furthermore, the preparation method in this study, which involved simple mixing of cement with MnO_2, resulted in a significantly smaller specific surface area than values reported in the literature (Tong, McNamara & Mayer 2019; Zhang et al. 2015). These factors collectively contributed to the limited degradation performance observed for $[benzene]_g$.

CO-REMOVAL FOR BENZENE AND H_2O_2

As shown in Figure 6, the NaOH+$MnSO_4$ and KI solutions demonstrated benzene removal efficiencies of 13% and 4%, respectively, while both achieved 94% $[H_2O_2]_g$ removal. The MnO_2 catalyst showed removal rates of 7% for benzene and 52% for $[H_2O_2]_g$. According to the results, the removal rate for $[benzene]_g$ by NaOH+$MnSO_4$ is almost equal to the value shown in Figure 5, which also proves that the influence of hydrogen bonding (main effect) mentioned earlier is reasonable. Combining the results shown in Figure 6, the decomposition rate of $[H_2O_2]_g$ by NaOH +$MnSO_4$ is stable compared with those in Figure 3. When benzene and $[H_2O_2]_g$ passed into the solution together, there were no coeffects between H_2O_2 and benzene in the solution. Figure 6 also shown that the $[benzene]_g$ removal rate by the MnO_2 catalyser is also stable compared with the data shown in Figure 5. All the results indicate that no effect contributed to the degradation of $[benzene]_g$ during the decomposition of $[H_2O_2]_g$. Conventional studies suggest that under alkaline conditions or manganese presence, the decomposition of hydrogen peroxide is

facilitated to generate hydroxyl radicals, which accelerate benzene oxidation and subsequently promote faster H_2O_2 breakdown. Kaur, Singh and Aggarwal (2024) also discovered that benzene oxidation through radical reactions could generate hydroxylated compounds, thereby influencing H_2O_2 decomposition. However, some studies have demonstrated inhibited H_2O_2 decomposition under excessively high pH conditions or through manganese speciation alterations (Opeida & Sheparovych 2019; Zhang et al. 2022). Given that the degradation rate of $[H_2O_2]_g$ remained consistently high in this experiment, it cannot be concluded that its decomposition was inhibited. However, it can be inferred that •OH radicals generated from 30% high-concentration H_2O_2 were not effectively utilized for pollutant degradation, but rather, as demonstrated in the following reaction equations, were quenched by H_2O_2 leading to accelerated self-decomposition (Cornu et al. 2022; Miller & Valentine 1995), even under specific conditions radicals become undetectable in reaction systems (Chirat, Viardin & Lachenal 1994; Nippatlapalli & Ganta 2024), and the oxidation potential of •OH diminishes with increasing pH (Ling et al. 2019), thus, led to the elimination of the synergistic effect, which constitutes a unique finding in this experimental study. Given that the $[H_2O_2]_g$ in this experiment originated from the 30% high-concentration H_2O_2 solution and the degradation solution maintained strong alkalinity, the aforementioned explanation remains chemically plausible.

$$H_2O_2 + \bullet OH \rightarrow HO_2\bullet + H_2O \quad (6)$$

$$HO_2\bullet + \bullet OH \rightarrow H_2O + O_2 \quad (7)$$

Although manganese dioxide (MnO_2) has been demonstrated to exhibit significant degradation effects on hydrogen peroxide (Elbasuney et al. 2024; Qi et al. 2021; Tian et al. 2000), Figure 6 simultaneously shows a decline in the removal efficiency of $[H_2O_2]_g$ by the catalyst. This decrease may be attributed to $[benzene]_g$ occupying the active sites on the particle surfaces, thereby hindering $[H_2O_2]_g$ access. Notably, the degradation rate of benzene remains low. This is because, as Jiang, Song and Zhu's (2021) study has indicated, the degradation efficiency of benzene by hydrogen peroxide alone is extremely limited (<2%) under co-existing conditions. Although MnO_2 particles can partially adsorb benzene, competitive adsorption leads to a sharp reduction in benzene adsorption efficiency compared to scenarios without H_2O_2. While hydroxyl radicals (•OH) generated from H_2O_2 decomposition could theoretically promote benzene degradation, these radicals

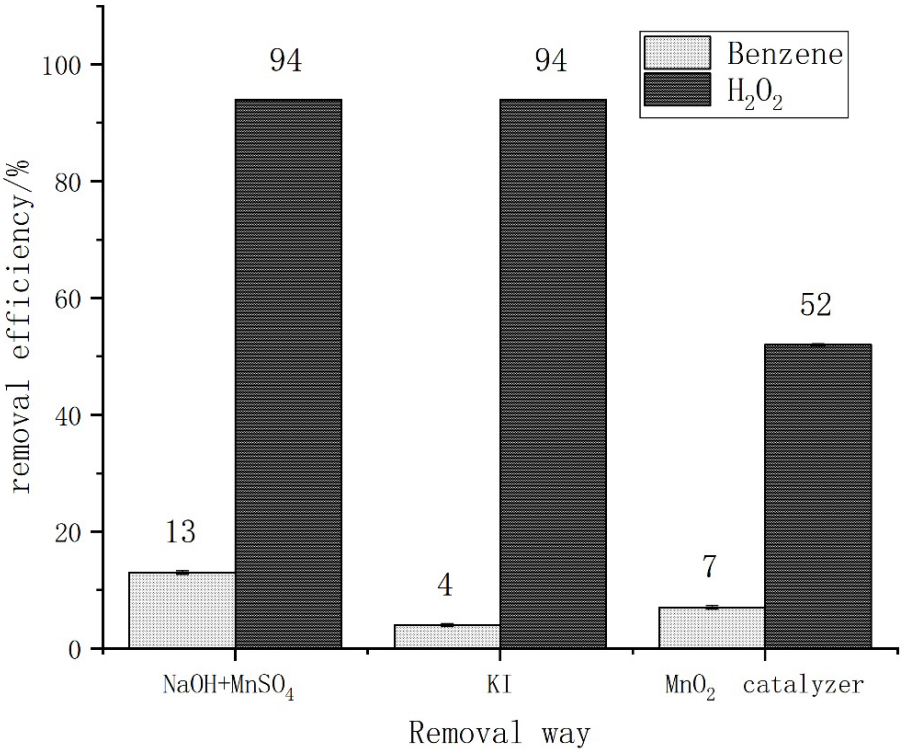

Conditions. The experimental conditions were the same as those used in Figure 1, except for the addition of 500 mL of removal reagent.

FIGURE 6. Co-removal of benzene and H_2O_2 in different ways

are confined to adsorption sites and cannot diffuse freely. Furthermore, as previously analyzed, the quenching effect of •OH radicals significantly limits their availability. Consequently, their contribution to benzene degradation is minimal, resulting in persistently low degradation rates. In addition, for KI solution, the $[H_2O_2]_g$ removal efficiency showed no decline compared to Figure 3, while the benzene removal rate plummeted from 32% in Figure 5 to 4% in Figure 6, which can also be interpreted as being due to the influence of hydrogen bonding effect. When $[H_2O_2]_g$ enters the KI solution, I^- was oxidized under acidic or neutral conditions (Ishita et al. 2023), the hydrogen bond-accepting capability of I^- with larger ionic radii diminishes, which led to a decrease in the effect, and then the solubility decrease. The experimental results obtained through three degradation methodologies employed in this study validate the previously proposed unique synergistic degradation hypothesis, demonstrating that under varying conditions synergistic effects may disappear, or lead to inhibited degradation of either $[H_2O_2]_g$. or $[benzene]_g$. This constitutes a systematic classification of synergistic effects.

MEASUREMENT OF pH

Due to the acidity of 30% H_2O_2, the neutrality of pure water and the alkalinity of the two solutions, the variation in the pH was monitored to investigate the interaction between H_2O_2 and benzene in the solutions, as shown in Figure 7. The work took a long time and could also avoid the possible interference in the sampling and determination process encountered in other detection methods, such as heating, adsorption and desorption. For pure water, the result shows that the pH in the opaque reactor is approximately accordant with 30% H_2O_2, which proves that no reaction occured under the condition, but under the irradiation of the adjacent UV lamp (5W, 253.7 nm), the value in the transparent reactor is increased to approximately 7, proving that H_2O_2 was completely decomposed. Based on previous studies by Jiang, Song and Zhu (2021), H_2O_2 decomposes under light irradiation to produce hydroxyl radicals (•OH), which in turn oxidize benzene into carbon dioxide and water. Additionally, the decomposition of hydrogen peroxide ultimately generates oxygen. For the $MnSO_4$+NaOH solutions, the results show that the pH values are similar to the initial value, which shows that although the solution was also contained in opaque reactors, the effects of catalysis and alkalinity were sufficient to degrade H_2O_2. Additionally, while some studies have also shown that the catalytic decomposition rate of hydrogen peroxide increases sharply under alkaline conditions (Ma et al. 2020; Shuhuan & Xinsheng 2010), it cannot be concluded that the pure catalytic decomposition rate is higher than that under pure alkaline conditions. After all, both alkaline and catalytic effects coexist in this study, and the efficient decomposition should be attributed to the combined action of the two factors. For KI solution, the pH is decreased with time because of the reduction of KI by the continuous oxidation of air and hydrogen peroxide. The rate of decrease of benzene shown in Figure 6 also confirms this phenomenon.

MEASUREMENT OF THE UV-Vis ABSORPTION

After the reaction, to clearly display the value for each absorption peak and the overall shape in the wavelength range, each peak is marked and all points are connected, as shown in Figure 8. It is obvious that for hydrogen peroxide (Figure 8(a)) and the mixture (Figure 8(b)), both

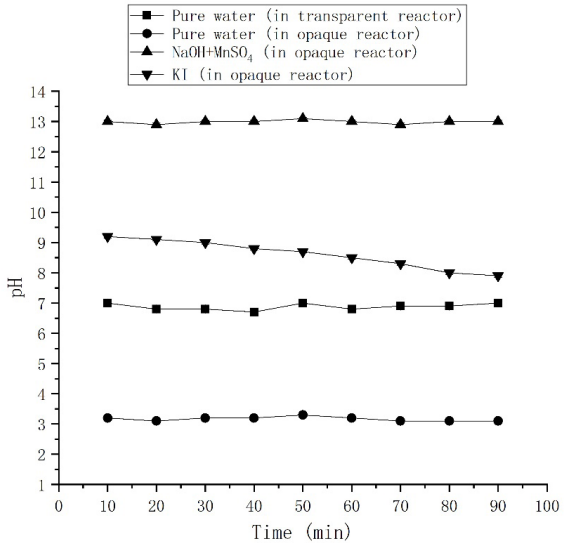

Conditions. The experimental conditions were the same as those used in Figure 1, except for the addition of 500 mL of removal reagent.

FIGURE 7. Variation in pH for the solution containing H_2O_2 and benzene

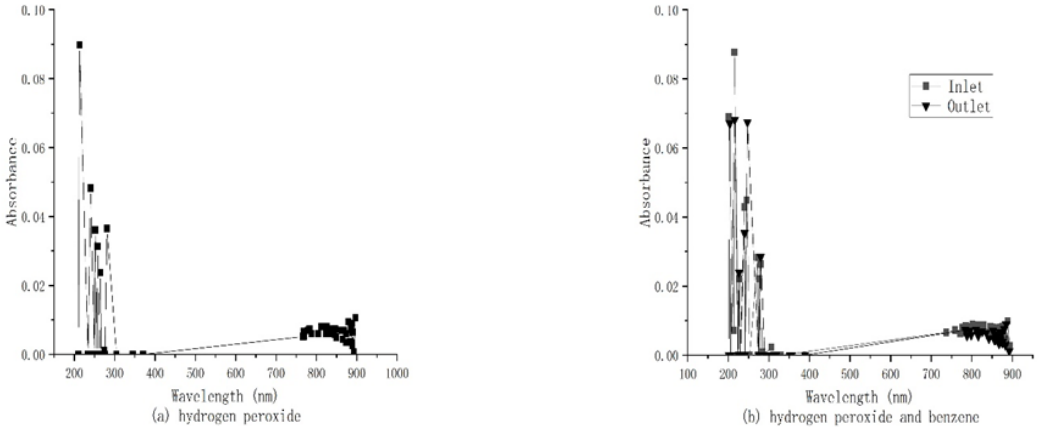

Conditions. The experimental conditions were the same as those used in Figure 1, except for the addition of 500 mL of removal reagent.

FIGURE 8. Absorption peak by UV–vis

the absorption peak and overall shape are very similar, which shows that because the amount of $[H_2O_2]_g$ is much larger than that of $[benzene]_g$, its absorption covers the typical bands of benzene (200-210 nm, 230-270 nm). In general, oxidants are always excessive in the oxidation reaction; therefore, interference should be considered. On the other hand, Figure 8(b) also shows more peaks than (a), which suggests that $[H_2O_2]_g$ can still oxidize $[benzene]_g$ to produce multiple intermediate products.

CONCLUSIONS

Solutions containing NaOH+$MnSO_4$ and KI, MnO_2 catalyst particles can degrade $[H_2O_2]_g$ and $[benzene]_g$. Under the condition of single existence for two substances, the thorough decomposition of $[H_2O_2]_g$ occurs and the removal of $[benzene]_g$ cannot be ignored due to the mechanism of alkalinity, catalysis and reducibility in which the main mechanism is assumed to involve the van der Waals force or hydrogen bond under different conditions. Analysis of pH changes has also raised a meaningful question: how to characterize the differences between the effects of alkalinity and catalysis on hydrogen peroxide decomposition? This requires further research. In the presence of $[H_2O_2]_g$ and $[benzene]_g$, this unique phenomenon - the lack of synergistic effects from H_2O_2 decomposition - could result from •OH radical scavenging under the combined influence of alkaline environment and elevated H_2O_2 concentration in the experiment. However, KI is oxidized by H_2O_2 in the solution, which leads to the reduction of hydrogen bonding interactions, leading to a significant decrease in benzene degradation rate. For the MnO_2 catalytic particles, it is speculated that the removal of $[benzene]_g$ will not be affected. In addition, oxidation by $[H_2O_2]_g$ can lead to a variety of intermediate products, and the characteristic absorption of excessive $[H_2O_2]_g$, which is the normal state of oxidation treatment, can cover that of the substrate. This study validates the initial hypothesis that $[H_2O_2]_g$-$[substrate]_g$ degradation exhibits distinct characteristics under varying conditions, demonstrating that even widely recognized mechanisms and principles cannot be universally applied. These findings highlight the necessity for more meticulous investigations.

ACKNOWLEDGEMENTS

This research was financially supported by the science project of Zhanshan City (Grant No. 2019B2015). The data used to support the findings of this study are included within the article.

REFERENCES

Chen, R., Wang, S., Cui, L., Liu, X., Zhang, W. & Pi, X. 2016. Synergy of FeMnOx and plasma for the removal of benzene. *Vacuum & Cryogenics* 22(3): 173-176. https://doi.org/10.3969/j.issn.1006-7086.2016.03.011

Chen, Y., Chi, Y., Wu, X., Lin, C., Lin, T., Gao, M., Zhao, C. & Sa, B. 2023. O-Vacancy-Rich ε-MnO_2 synthesized at hydrophobic interface: An efficient Fenton-like catalyst for removing ciprofloxacin from water. *Crystals* 13(12): 1664. https://doi.org/10.3390/cryst13121664

Chen, Z., Chen, S., Gong, Y., Shen, H. & Xu, X. 2020. Partitioning of hydrogen peroxide in gas-liquid and gas-aerosol phases. *Atmospheric Chemistry and Physics* 20(5): 5513-5526. https://doi.org/10.5194/acp-20-5513-2020

Chirat, C., Viardin, M.T. & Lachenal, D. 1994. Use of a reducing stage to avoid degradation of softwood kraft pulp after ozone bleaching. *Paperi ja Puu* 76(6/7): 409-418.

Cornu, D., Coustel, R., Durand, P., Carteret, C. & Ruby, C. 2022. How can pH drop while adding NaOH? Formation and transformation of $Mn_4(OH)_6SO_4$. *Journal of Solid State Chemistry* 305: 122631. https://doi.org/10.1016/j.jssc.2021.122631

Elbasuney, S., Attwa, M., Deif, A., ElGamal, M., Fayoud, A., Abdelkhalek, S.M. & Gobara, M. 2024. Green synthesis and catalytic activity assessment of bespoke nano-catalyst for eco-friendly green propellant systems based on hydrogen peroxide. *Brazilian Journal of Chemical Engineering* 41: 1151-1164. https://doi.org/10.1007/s43153-023-00380-5

Fuku, K., Kanai, H., Todoroki, M., Mishima, N., Akagi, T., Kamegawa, T. & Ikenaga, N. 2021. Heterogeneous Fenton degradation of organic pollutants in water enhanced by combining iron-type layered double hydroxide and sulfate. *Chemistry - An Asian Journal* 16(14): 1887-1892. https://doi.org/10.1002/asia.202100375

Ishita, I., Sahoo, P., Sow, P.K. & Singhal, R. 2023. Unlocking the potential of KI as redox additive in supercapacitor through synergistic enhancement with H_2SO_4 as a co-electrolyte. *Electrochimica Acta* 451: 142286. https://doi.org/10.1016/j.electacta.2023.142286

Jiang, Y., Song, J. & Zhu, A. 2021. Gas-phase advanced oxidation (GPAO) for benzene-containing gas by an ultraviolet irradiation/hydrogen peroxide vapour (UV/[H_2O_2]g) process. *Environmental Science and Pollution Research* 29(11): 16418-16426. https://doi.org/10.21203/rs.3.rs-218136/v1

Kaur, P., Singh, D. & Aggarwal, S.G. 2024. Benzene: A critical review on measurement methodology, certified reference material, exposure limits with its impact on human health and mitigation strategies. *Environmental Analysis Health and Toxicology* 39: e2024012. https://doi.org/10.5620/eaht.2024012

Kim, K.M., Kim, I.G., Nam, Y.S., Choi, J., Chung, W., Oh, I., Lee, K.B., Jung, M., Park, S. & Nam, I.W. 2018. Catalytic decomposition of hydrogen peroxide aerosols using granular activated carbon coated with manganese oxides. *Journal of Industrial and Engineering Chemistry* 62: 225-233. https://doi.org/10.1016/j.jiec.2017.12.062

Kumar, A., Holuszko, M.E. & Janke, T. 2020. Removal of flame retardants from the non-metal fraction of the processed waste printed circuit boards using organic solvents and pyrolysis. *Environmental Engineering and Management Journal* 19(6): 907-916. https://doi.org/10.30638/eemj.2020.086

Li, J., Li, H., Wang, X., Wang, W., Ge, M., Zhang, H., Zhang, X., Li, K., Chen, Y. & Wu, Z. 2021a. A large-scale outdoor atmospheric simulation smog chamber for studying atmospheric photochemical processes: Characterization and preliminary application. *Journal of Environmental Sciences* 102: 189-198. https://doi.org/10.1016/j.jes.2020.09.015

Li, P., Yang, C., Zhang, C., He, G., Xu, C., Liu, J., Li, C., Zhang, Y., Sun, Y., Li, X., Wang, X., Chen, J., He, H., Herrmann, H. & Mu, Y. 2021b. Photochemical aging of atmospheric fine particles as a potential source for gas-phase hydrogen peroxide. *Environmental Science & Technology* 55(22): 15063-15068. https://doi.org/10.1021/acs.est.1c04453

Li, T., Simon, L.C. & Jonathan, P.D.A. 2020. Fast oxidation of sulfur dioxide by hydrogen peroxide in deliquesced aerosol particles. *PNAS* 117: 1356-1362. https://doi.org/10.1073/pnas.1916401117

Ling, L., Cui, L., Huang, F., Chen, M., Zeng, G., Huang, D., Lai, B., Liu, S., Zhang, M., Qin, L., Li, M., He, J., Zhao, Y. & Chen, L. 2019. Degradation of naphthalene with magnetic bio-char activate hydrogen peroxide: Synergism of bio-char and Fe-Mn binary oxides. *Water Research* 160: 238-248. https://doi.org/10.1016/j.watres.2019.05.081

Liu, L., Liu, G., Ruan, F., Xin, X., Zhang, L. & Duan, H. 2025. Enhanced anaerobic sludge digestion by calcium peroxide pretreatment combined with manganese dioxide: Performances and mechanisms. *ACS ES&T Water* 5(1): 1-12. https://doi.org/10.1021/acsestwater.4c01225

Luan, S.L., Tavares, M.D., Zanin, J.A., Hidalgo, M.T. & Dias, L.A. 2021. Implications of COD analysis use in the peracetic acid-based wastewater treatment. *Water Science & Technology* 84(5): 1270-1278. https://doi.org/10.2166/wst.2021.300

Ma, J., Yu, X., Jiang, X., Wang, J., Li, J., Zhang, Y., Chen, L. & Wang, Y. 2020. Percarbonate persistence under different water chemistry conditions. *Chemical Engineering Journal* 389: 124342. https://doi.org/10.1016/j.cej.2019.123422

Miller, C.M. & Valentine, R.L. 1995. Oxidation behavior of aqueous contaminants in the presence of hydrogen peroxide and filter media. *Journal of Hazardous Materials* 41(1): 105-116. https://doi.org/10.1016/0304-3894(94)00098-2

Möller, D. 2009. Atmospheric hydrogen peroxide: Evidence for aqueous-phase formation from a historic perspective and a one-year measurement campaign. *Atmospheric Environment* 43(38): 5930-5937. https://doi.org/10.1016/j.atmosenv.2009.08.013

Nippatlapalli, N. & Ganta, A. 2024. Recent progress on application of nonthermal plasma for the degradation of aqueous emerging contaminants: A review on mechanism, reactor strategies, integrated systems and future perspective. *Process Safety and Environmental Protection* 187: 1454-1470.

Opeida, I.A. & Sheparovych, R.B. 2019. Inhibition by hydrogen peroxide in the radical chain oxidation of hydrocarbons by molecular oxygen. *Theoretical and Experimental Chemistry* 55(1): 36-42. https://doi.org/10.1007/s11237-019-09593-7

Qi, X., Sun, X., Yang, H., An, H., Li, F., Xu, W. & Wang, Y. 2021. Solubilities of benzene, toluene, and ethylbenzene in deep eutectic solvents. *Journal of Chemical & Engineering Data* 66(6): 2460-2469. https://doi.org/10.1021/acs.jced.1c00091

Quentin, H., Bellenoue, B., Boust, M., Bouchez, R. & Batonneau, Y. 2022. Experimental comparison of hydrogen peroxide catalysts for a hydrogen peroxide/n-decane bipropellant combustor. *Journal of Propulsion and Power* 38(2): b38593. https://doi.org/10.2514/1.b38593

Shuhuan, M. & Xinsheng, C. 2010. Kinetics of Mn^{2+}-induced hydrogen peroxide decomposition in alkaline medium. In *Research Progress in Paper Industry and Biorefinery* (4th ISETPP), Vols 1-3. https://doi.org/10.0410/cata/6819d30dcd134093f02b457d1309ccd7

Singh, H., Singh, D. & Mishra, A.K. 2019. Multi-objective particle swarm optimization-based adaptive neuro-fuzzy inference system for benzene monitoring. *Neural Computing & Applications* 31(5): 2195-2201. https://doi.org/10.1007/s00521-017-3181-7

Tian, H., Zhang, T., Yang, H., Sun, X., Liang, D. & Lin, L. 2000. Manganese-lead mixed oxide catalysts for decomposition of hydrogen peroxide. *Chinese Journal of Catalysis* 21(6): 600-602.

Tong, Y., McNamara, P.J. & Mayer, B.K. 2019. Adsorption of organic micropollutants onto biochar: A review of relevant kinetics, mechanisms and equilibrium. *Environmental Science: Water Research & Technology* 5(5): 821-832. https://doi.org/10.1039/C8EW00938D

Villanueva, A.D. 2018. Salting out and salting in of benzene in water: A consistency evaluation. *Monatshefte für Chemie* 149: 231-242. https://doi.org/10.1007/s00706-017-2122-6

Wang, T. 2012. New method for removal of hydrogen peroxide interference in the analysis of chemical oxygen demand. *Environmental Science & Technology* 46(4): 2294-2302.

Wang, Y., Hou, Y., Wu, W., Liu, D., Ji, Y. & Ren, S. 2016. Roles of a hydrogen bond donor and a hydrogen bond acceptor in the extraction of toluene from n-heptane using deep eutectic solvents. *Green Chemistry* 18(8): 3089-3098. https://doi.org/10.1039/c5gc02909k

Xu, X., Zhang, X., Liu, S., Zhang, J. & Xu, Y. 2018. Sustained production of H_2O_2 in alkaline water solution using borate and phosphate-modified Au/TiO_2 photocatalysts. *Photochemical & Photobiological Sciences* 17: 102-108. https://doi.org/10.1039/c8pp00177d

Xuan, X., Chen, Z., Gong, Y., Shen, H. & Chen, S. 2020. Partitioning of hydrogen peroxide in gas-liquid and gas-aerosol phases. *Atmospheric Chemistry and Physics* 20(9): 5513-5526. https://doi.org/10.5194/acp-20-5513-2020

Zhang, G., Ren, L., Yan, Z., Kang, L., Lei, Z., Xu, H., Shi, F. & Liu, Z.H. 2015. Mesoporous-assembled MnO_2 with large specific surface area. *Journal of Materials Chemistry A* 3: 13263-13271. https://doi.org/10.1039/C5TA01399D

Zhang, H., Wang, H., Huang, H., Li, Y., Liu, J. & Zhang, X. 2018. Cooperative decomposition of hydrogen peroxide by lignin-combined transition metals in pulp bleaching. *BioResources* 13(2): 3922-3932. https://doi.org/10.15376/biores.13.2.3922-3931

Zhang, X., Liu, Y. & Lu, R. 2010. Decomposition kinetics and mechanism of alkaline hydrogen peroxide with transition metals. *Journal of South China University of Technology (Natural Science Edition)* 38(9): 40-45. https://doi.org/10.3969/j.issn.1000-565X.2010.09.008

Zhang, X., Zhou, B., Yin, S., Wang, Y., Zhang, X., Meng, Q., Meng, F., Wei, C. & Wen, G. 2022. Mesoporous manganese dioxide prepared by nano-casting: An efficient catalyst for degradation of methyl orange and oxalic acid in aqueous solution. *Vacuum* 206: 111495. https://doi.org/10.1016/j.vacuum.2022.111495

*Corresponding author; email: jyp@zsc.edu.cn